

ARTICLE



Piperazine and methyldiethanolamine interrelationships in CO₂ absorption by aqueous amine mixtures. Part II—Saturation rates of mixed reagent solutions

Camilla Costa¹ | Renzo Di Felice² | Paolo Moretti¹ | Maddalena Oliva¹ | Rouzbeh Ramezani²

¹Dipartimento di Chimica e Chimica Industriale, Università degli Studi di Genova, Genoa, Italy

²Dipartimento di Ingegneria Civile, Chimica ed Ambientale, Università degli Studi di Genova, Genoa, Italy

Correspondence

Camilla Costa, Dipartimento di Chimica e Chimica Industriale, Università degli Studi di Genova, Via Dodecaneso 31, 16146 Genoa, Italy.
Email: camilla.costa@unige.it

Abstract

This work is a companion to a previous article, Part I, published in *The Canadian Journal of Chemical Engineering*, dealing with CO₂ absorption in aqueous solutions containing a single aminic reagent (specifically methyldiethanolamine (MDEA) or piperazine (PZ)). In this second part, different PZ/MDEA mixtures are experimentally studied and their performances are compared with that of the single reagents. It is indeed well known that small quantities of PZ added to MDEA aqueous solutions are sufficient to obtain a significant improvement in the kinetics of the process. PZ is considered an activator or promoter for MDEA, but the mechanism of this synergy has still not been clearly demonstrated. The aim of this study is an attempt to understand how PZ and MDEA can interact by experimentally analyzing this beneficial mutual effect and by explaining it with the help of a suitable yet not complex model. We believe that the involved chemistry is not more complex than that reported in Part I for the single reagents. According to our findings, it is MDEA that enhances the action of PZ, as opposed to what many authors claim. Moreover, our results seem to rule out the existence of any PZ shuttle effect.

KEYWORDS

activated MDEA, amine blend, CO₂ capture, MDEAa, mixed absorbents

1 | INTRODUCTION

Blended aminic absorbents containing a primary (or secondary) amine and a tertiary amine are actively studied for carbon dioxide (CO₂) removal. This is because they can combine the desirable properties of the individual components, in particular the high rate of reaction of the primary or secondary amine and the low enthalpy of reaction of the tertiary amine. Aqueous solutions of PZ-activated MDEA, aMDEA for short, were invented and patented by BASF as gas scrubbing agents, separating CO₂ more efficiently than the traditional

monoethanolamine or potassium carbonate reagents.^[1] BASF originally used the aMDEA technology in its own ammonia and syngas plants only, but then started licensing it to other ammonia manufacturers and oil and gas companies.

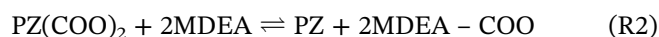
In spite of the widespread industrial utilization of aMDEA, the works available in the scientific literature are relatively few and, more importantly, the mechanisms of interaction between MDEA and PZ are even today not elucidated. Different hypotheses were formulated but none has been adequately verified yet.

Several studies have been carried out on the thermodynamic equilibrium of the PZ/MDEA systems and a qualitative consensus exists.^[2–10] Along with thermodynamics, the kinetic behaviour of the system, namely the overall CO₂ absorption rate, has also been investigated by various authors.^[11–21] In particular, we are strongly interested in the possible existence of a PZ regeneration mechanism sustaining a long-term enhanced absorption rate, as claimed by several authors. A concise review of this subject is presented below.

Xu et al.^[11] who used a disc column to investigate the kinetics of carbon dioxide absorption, assert that MDEA may react with CO₂ to form an unstable complex MDEA - COO. Then the hydrolytic reaction of MDEA-COO takes place:

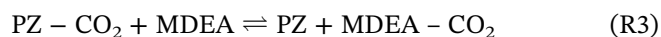


Simultaneously, PZ can react rapidly to form the intermediate PZ(COO)₂. PZ should act as an activator because it could transfer CO₂ to MDEA as follows:



In addition, PZ can be renewed, following a so-called shuttle mechanism.

A similar mechanism is used by Zhang et al.^[12] who investigated the system by a disc column. According to these authors, PZ can transfer CO₂ to MDEA as a homogeneous activator as follows:



Therefore, the CO₂ absorption is promoted and at the same time PZ can regenerate itself.

Weiland et al.^[14] studying the action of PZ on MDEA, affirm that most of the CO₂ reacts with PZ since it is unable to react with MDEA. The reaction product (the PZ carbamate) then continues to diffuse into the bulk liquid and eventually it dissociates, forming PZ (which diffuses back towards the interface) and CO₂ (ie, converted into HCO₃⁻).

Ibrahim et al.^[18] modelled the absorption process on a simulator to study the effect of using PZ as an activator. According to the authors, PZ acts as a shuttle that quickly reacts with CO₂ to reduce the resistance to mass transfer, and then passes on the CO₂ to MDEA. In this way PZ becomes available yet again.

Ying et al.^[21] also assert that PZ can regenerate itself when mixed with MDEA. They used a semi-batch stirred cell with CO₂ continuous operation to investigate the activation mechanism of PZ in aqueous MDEA solutions and found that PZ regeneration seems to be present in the long timescale of the experiments.

From the above discussion it can be noted that some authors, when describing the system behaviour, introduce quite arbitrary reactions in the reaction pathway related to a hypothetical shuttle mechanism. The intermediates involved in these reactions, however, have never been isolated or detected. Other authors, without going into detail about the mechanism, invoke the ability of PZ to regenerate itself, working as a shuttle agent. These justifications used to explain the absorption process enhancement produced by PZ addition seem unconvincing to us and in any case they have never been conclusively proven.

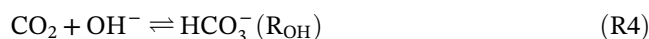
The aim of this work is to understand how PZ and MDEA can interact when mixed in aqueous solutions for CO₂ absorption, in order to find a reasonable explanation for the synergistic effects that are characteristic of this important solvent.

As in Part I,^[22] this work includes an experimental investigation of the absorption rate of CO₂ into aqueous MDEA + PZ solutions at different reagent concentrations and different CO₂ loadings. The absorbing device, a hollow fibre membrane contactor, and the operating conditions are identical to those used in Part I in order to facilitate accurate comparisons. A simple and manageable model is used as a support to meaningfully interpret the experimental evidence.

2 | BACKGROUND

It is important to point out that the effect of various additives, including amines, added in small quantities to absorbent solutions has been studied for a long period of time. However these studies, which have been conducted since the 1920s,^[23,24] have mainly dealt with potassium carbonate solutions, which have been and are among the most popular chemical absorbents, especially for bulk CO₂ removal. The addition of potassium carbonate to water is simply a way to introduce a strong base, OH⁻, into the liquid absorbent. Additionally, a buffer system carbonate/bicarbonate is created in this way.

In a basic study conducted by Shrier and Danckwerts,^[25] a number of amines were used to promote CO₂ absorption in potash, the most effective being 2-ethylaminoethanol. This effect is due to the presence of a buffer solution in the bulk liquid, where the fraction of the total amine present in free form can be expressed in terms of the buffer ratio [HCO₃⁻]₀/[CO₃²⁻]₀ (subscript 0 refers to initial conditions before any CO₂ absorption). The overall absorption rate in ordinary carbonate solutions,^[26] at pH > 10, is determined by the dominant reaction:



The rate of this dominant reaction is low due to the low hydroxyl ion concentration. Ethanolamine added in

the potash solution can work as a carrier of CO₂ from the surface region into the bulk liquid. It is well known that for many primary and secondary amines the rate of the reaction with CO₂ is high^[27]



The amine itself can also function as a basis for capturing the proton produced by Reaction (R5):



In a buffered solution, simple considerations related to the involved chemical equilibrium indicate that a certain fraction of the amine can exist in the free form (RR'NH) and can produce more rapid CO₂ capture by the R_{Am} reaction relative to reaction R_{OH}. Therefore, in the surface region the contribution of the reaction between CO₂ and OH⁻ ion is negligible and is roughly as follows:

$$\frac{k_{\text{Am}}[\text{RR}'\text{NH}]}{k_{\text{OH}}[\text{OH}^-]} \sim 10 - 1000 \quad (1)$$

However, the reversion of the carbamate ion to bicarbonate ion is known to be slow. Therefore, in order to react significantly, the carbamate ion must diffuse to the liquid bulk, where free amine is regenerated as reaction R_{Am} proceeds in the reverse direction, since CO₂ is consumed through reaction R_{OH}. The fresh amine then diffuses back to the interface (shuttle mechanism). A sustained improvement in the overall absorption rate can be obtained if reaction R_{OH} in the bulk liquid is fast.

The authors highlight that the addition of amine has a beneficial lasting effect in buffered carbonate/bicarbonate solutions, while this does not occur with ordinary amine solutions wherein free amine is progressively converted to unreactive forms.

Astarita et al^[28] published another fundamental work containing a general analysis of the promotion of the mass transfer rate in a system formed by CO₂, potassium carbonate, water, promoter. They provided a clear definition of rate promoter. Inorganic additives act as homogeneous catalysts as they enhance the overall rate of absorption without undergoing any chemical transformation. Instead, the amino compounds act by way of a shuttle mechanism. We would stress that caution must be used when the shuttle mechanism is called upon.

In classical treatments of the absorption process, chemical equilibrium is always assumed to prevail in the bulk of the liquid. If a reaction is fast enough to enhance the mass transfer rate, it will be fast enough to maintain chemical equilibrium in the bulk. However, in the case of

a shuttle mechanism, the reaction causing the rate enhancement is not the same reaction that is required to be at equilibrium in the bulk. Astarita and coworkers^[28] sketch the situation as follows:



The difference between the homogeneous catalysis and the shuttle mechanism is only related to the relative rate of step (2B), while step (2A) is rapid in any case. For the former system, (2B) is so much faster than (2A) that it follows immediately and locally. For the latter, (2B) is so much slower that it can only take place in the bulk of the liquid; therefore, diffusion also must occur. Chemical equilibrium is established in the bulk only if step (2A) is sufficiently fast, despite its intrinsic slowness (rate-controlling step).

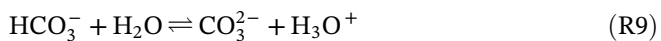
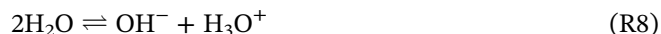
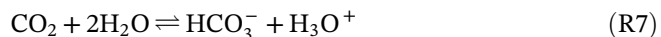
The important considerations summarized above in the pioneering works by Shrier and Danckwerts^[25] and Astarita and coworkers^[28] are specifically tailored for potassium carbonate solutions only. However, in a rather arbitrary way, in the more recent literature this interpretation of the system behaviour has been sometimes extended to blends formed by two or more amines and no longer containing potassium carbonate. In several articles the terms “promoter,” “activator,” or “shuttle” are used for PZ though sound ambiguous or remain virtually unexplained.

Three PZ/MDEA/water blends were studied here, named A, B, and C, with the aim of investigating and possibly clarifying PZ and MDEA interrelationships. With respect to blend A, B was selected for elucidating the effect of a higher PZ concentration and C for observing the effect of the MDEA concentration, which has a marked influence on the solution viscosity. The compositions of A, B, and C are summarized in Table 1.

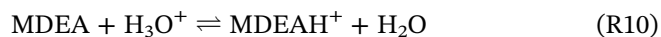
The following chemical reactions have all been observed in studies involving a single absorbent (either MDEA or PZ); therefore, they will unquestionably occur when absorbing PZ/MDEA/water blends come into contact with CO₂. Next to the classical carbonation reactions and water dissociation:

TABLE 1 Composition of the three PZ/MDEA/water blends investigated

Mixture	PZ content		MDEA content	
	w/w	molarity	w/w	molarity
A	1%	0.116	10%	0.844
B	2%	0.233	10%	0.844
C	1%	0.116	30%	2.580



if MDEA is present it will protonize



if PZ is present it will react with CO_2 to form carbamate



which can react further to form dicarbamate



next to PZ and its carbamate protonation



In order to limit the number of chemical species to be included in the discussion of those that are significantly influential, the equilibrium reaction leading to the formation of diprotonated piperazine (PZH_2^{2+}) was not included. This assumption is justified by Derks and coworkers.^[29] Indeed, at 25°C the second pK_a of piperazine to form diprotonated piperazine is 5.35 (vs 9.73 for the first pK_a ^[30]) and then low enough that the related equilibrium can be neglected.

According to Bishnoi and Rochelle,^[31] the equilibrium constant for the reverse of reaction (R14) can be

expressed through a pK_a for piperazine carbamate. They suggest the value 9.48 at 25°C.

The important issue at the centre of the matter under discussion is whether additional chemical equations are necessary to correctly describe the system behaviour, such as the introduction of a shuttle mechanism involving PZ as CO_2 carrier towards MDEA.

3 | MATERIALS AND METHODS

A gas mixture (supplied by Air Liquide Italia) containing 15% (mol/mol) of carbon dioxide with nitrogen as balance was used as feed gas.

The aqueous absorbing solutions are prepared at the desired concentration by dissolving known amounts of reagents in deionized water. The selected reagents methyldiethanolamine (MDEA) $\geq 99\%$ and piperazine (PZ) $\geq 99\%$ were purchased from Aldrich.

Figure 1 shows a schematic sketch of the experimental set up, based on a hollow fibre membrane contactor,^[32,33] where CO_2 is transferred from gas to liquid. Part I provides more detail.^[22]

It must be stressed that in this work the membrane contactor is purely the selected absorbing device, already

TABLE 2 Operating conditions for the CO_2 absorption tests

Temperature	25°C
Pressure	Ambient
CO_2 content in the feed gas	15% mol/mol
Gas rate	$8 \cdot 10^{-6} \text{ m}^3/\text{s}$
PZ concentration	1% w/w-2% w/w
MDEA concentration	10% w/w-30% w/w
CO_2 loading	0-0.8

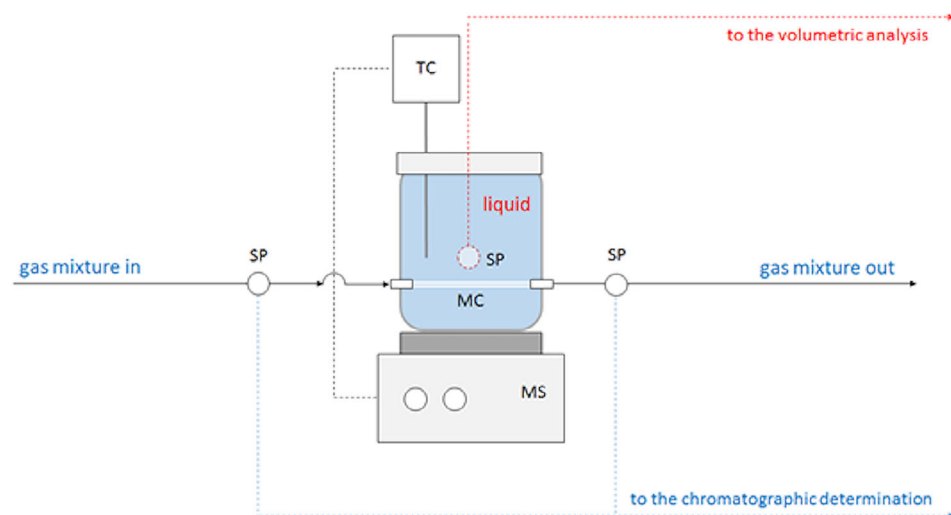
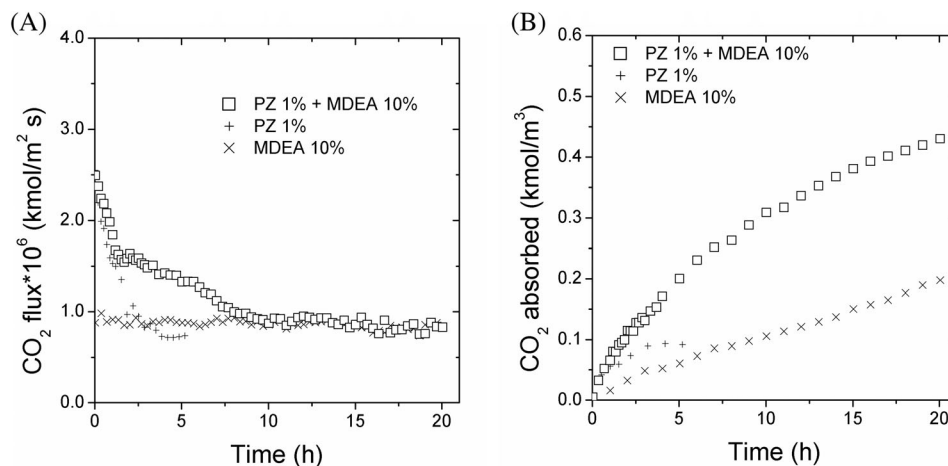
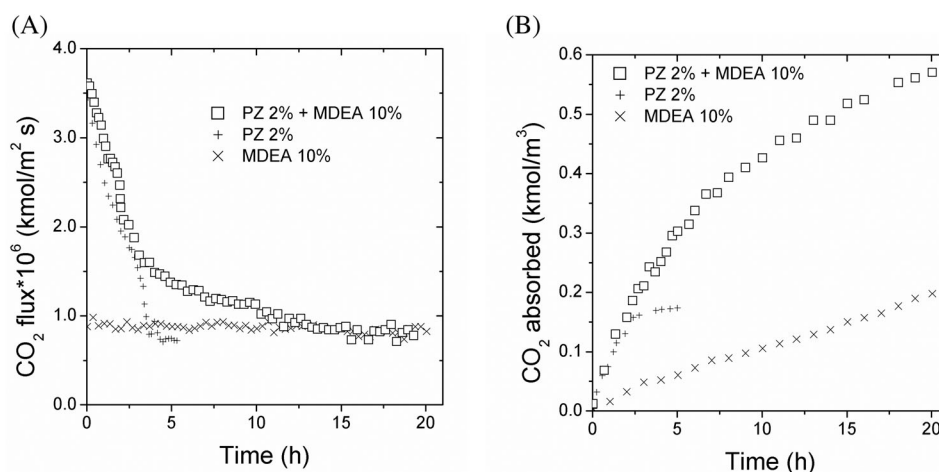


FIGURE 1 Simplified setup for absorption of CO_2 in aqueous amine solutions. MC, membrane contactor; MS, magnetic stirrer; SP, sampling point; TC, temperature controller

FIGURE 2 CO₂ absorption performance of mixture A with time**FIGURE 3** CO₂ absorption performance of mixture B with time

characterized in Part I, and the focus is not on the membrane (an inert support stabilizing the gas/liquid interface) but on the behaviour of the absorbing solution. The module, built in-house, consists of four microporous hollow fibres made of polypropylene, with nominal porosity 60%, an average pore size 0.2 μm , and supplied by Membrana (Germany).^[34,35]

The adopted arrangement is continuous in the gas phase, which flows into the fibre lumen, and discontinuous in the liquid phase, which is contained in a cylindrical glass vessel and mixed by a magnetic stirrer. The liquid temperature is maintained at 25°C (within $\pm 1^\circ\text{C}$) by a temperature controller. The time required for a single test was quite long, as the gas was allowed to flow at constant flow rate for several hours in order to gradually saturate the absorbing solution.

The system behaviour was monitored in terms of the: (a) gas phase side, as well as (b) liquid phase side, as illustrated below.

The gas composition (a) was continuously analyzed using an Agilent 490 microGC equipped with a PorapLOT U column and a thermal conductivity detector (TCD). The CO₂ absorption rate, expressed in kmol/

(m² · s), was estimated at any time by performing a gas side mass balance over the contactor as follows:

$$J_{\text{CO}_2} = \frac{v(C_{\text{CO}_2,\text{in}} - C_{\text{CO}_2,\text{out}})}{A} \quad (2)$$

where $C_{\text{CO}_2,\text{in}}$ is the CO₂ concentration (kmol/m³) in the gas phase at the inlet of the contactor (feed gas); $C_{\text{CO}_2,\text{out}}$ is the CO₂ concentration in the gas phase at the outlet (treated gas); A (m²) is the interfacial area useful for the mass transfer; and v is the gas flow rate (m³/s). The estimated expanded uncertainty for the CO₂ absorption flux measurements was $5 \cdot 10^{-8}$ kmol/(m² · s).

Liquid samples (b) were periodically withdrawn without significant depletion of the liquid volume and analyzed in order to evaluate the total loading α , that is, the ratio of moles of CO₂ captured (comprising aqueous CO₂, carbamate species, bicarbonate, and carbonate) to total initial moles of amines. This was determined based on a volumetric method (see Part I) that facilitates the measurement of the CO₂ volume developed by hydrochloric acid reacting with a known volume of loaded solution.

The CO₂ volume was obtained using the following formula:

$$V_{CO_2} = \frac{V_t(P_t - p_w) \times 273}{760 \times (T + 273)} \quad (3)$$

where V_t is the volume of evolved gas in cm³; P_t is the ambient pressure in mm Hg; T is the liquid temperature in °C; and p_w is the vapour pressure of the liquid in mm Hg at temperature T . From V_{CO_2} the moles of CO₂ absorbed into the liquid and the total loading are easily calculated. The estimated expanded uncertainty for measurements of the loading was 0.05.

The viscosities of the absorbing solutions were determined by means of Ubbelohde capillary viscometers coupled with a pycnometer equipped with a thermometer. A water bath maintained the desired temperature (within $\pm 0.5^\circ\text{C}$) during the measurements. The estimated expanded uncertainty for the viscosity measurements was 0.05 mPa · s.

The operating conditions selected in this work are collected in Table 2.

4 | RESULTS AND DISCUSSION

In order to clarify the PZ/MDEA interactions as much as possible, the experimental results obtained from mixtures A, B, and C (see Table 1) are presented and discussed. In Figures 2 and 3 the raw data collected under the conditions illustrated in Table 2 are reported for systems A and B, respectively.

The change in the CO₂ absorbing rate with time was measured following procedure (a) by analyzing the gas phase side, and the moles of CO₂ progressively captured in the liquid solution were measured through procedure (b) by analyzing the liquid phase side.

In every graph, the mixture behaviour was compared with that of the two standalone components.

Figures 2 and 3 show that when PZ is the only reagent the absorption flux rapidly declines with time and at a certain time $t_{max} \approx 3\text{--}4$ hours it drops to the absorption rate of pure water ($\sim 0.8 \cdot 10^{-6}$ kmol/m² · s in our system). After this time interval the experiment was stopped. This happens because after 3 to 4 hours all the reactive PZ, and its carbamate, in the liquid solution are consumed; therefore, the effect due to reactions (R11) and (R12) on the overall transfer process rate becomes negligible. The interplay of reactions (R11)–(R14) at different loadings is not discussed here. An interesting and detailed discussion about this subject can be found in recent work by Stowe and

cowerkers,^[36] who used combined ab initio and classical force field calculations. The authors recall that CO₂ absorption occurs through the reaction with not only PZ (R11) but also PZCOO[−] (R12) and that the absorption rate will be a function of their relative availability. PZ and PZCOO[−] may also act as proton acceptors (R13 and R14), while PZH⁺ further protonation hardly takes place.^[29] The production of H⁺PCOO[−] is found to be more probable with the increase in CO₂ loading, and this transfer can liberate a certain amount of fresh PZ. Returning to our results, the final stabilization of the CO₂ flux at $\approx 0.8 \cdot 10^{-7}$ kmol/m² s takes place near the thermodynamic equilibrium of our system. In fact, the PZ 1% solution (Figure 2B) exhibits, at the time t_{max} mentioned above, a maximum number of kmol/m³ of CO₂ captured ≈ 0.095 , while the PZ 2% solution (Figure 3B) reaches a value ≈ 0.195 . These measurements translate into a maximum CO₂ loading of roughly $0.095/0.116 = 0.82$ for the first solutions, and a maximum CO₂ loading of roughly $0.195/0.233 = 0.84$ for the second solution, which can be compared with an equilibrium loading of 0.85 for a CO₂ partial pressure of 15 kPa at 25°C.^[22]

The study of the solutions where MDEA is the only reagent (Figures 2, 3, and 9) provides the same information from all the cases considered. The absorption flux remains constant during the entire time interval explored, at a level (of the order of $0.9 \cdot 10^{-6}$ – $1 \cdot 10^{-6}$ kmol/m² · s) only slightly higher than that measured for pure water. As detailed in Part I,^[22] this is due to the fact that the kinetic constant for the overall reaction of CO₂ with MDEA (R1 + R4):



is too small (four orders of magnitude lower than that of PZ (R5 + R7)^[37,38]) to make a significant contribution to the overall absorption rate; the small positive effect on the absorption rate generated by an enhanced MDEA concentration (see Figure 9) is balanced by the negative effect caused by the increase in viscosity, with a reduction of the liquid side mass transfer coefficient k_L . In this case, no t_{max} was detected during the experimental runs since the time span was insufficient to reach the thermodynamic equilibrium between the gas phase and liquid phase. Accordingly, the number of moles of CO₂ that accumulates in the liquid increases steadily (see Figures 2B, 3B, and 9B).

It is important to remark that the above considerations extracted from gas side measurements closely match those extracted from the liquid side, although the two measurements are totally independent from each other.

FIGURE 4 Component speciation in the bulk liquid phase for: A, PZ 1% and blend A; and B, PZ 1% + MDEA 10% at different loadings

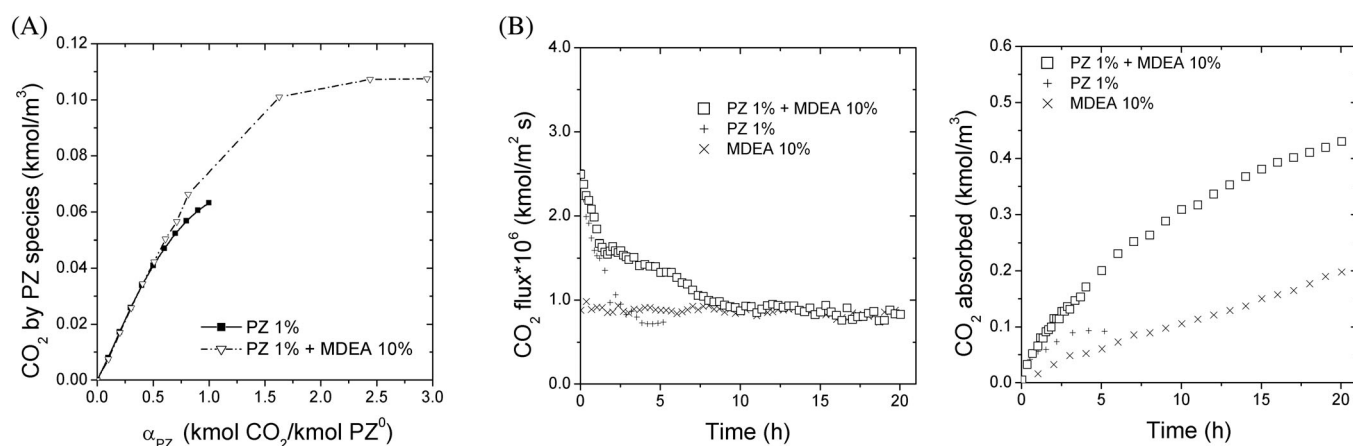
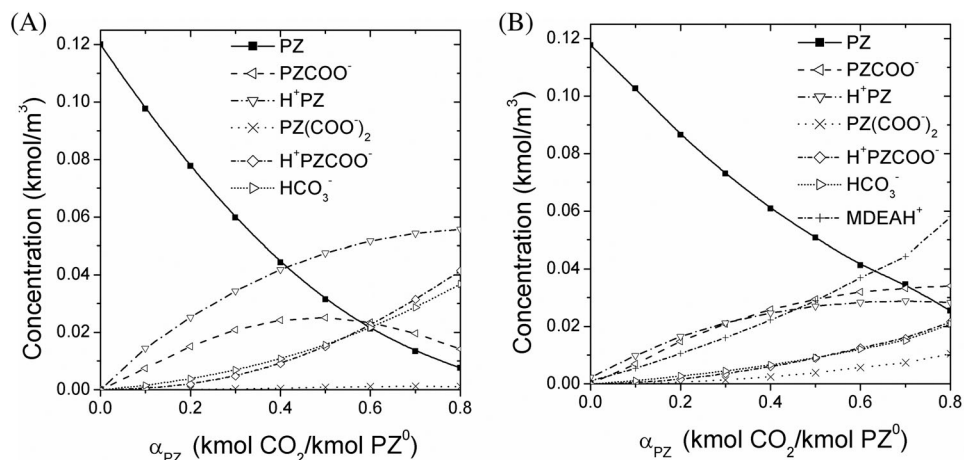


FIGURE 5 CO₂ captured by PZ 1% with and without MDEA from: A, predicted speciation; and B, experimental measurements

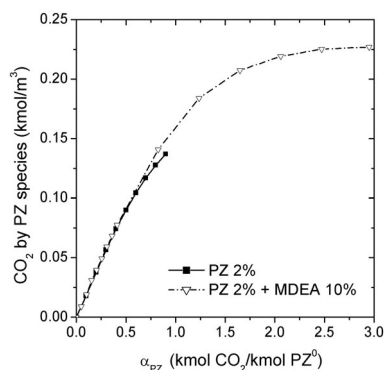


FIGURE 6 CO₂ captured by PZ 2% with and without MDEA

In summary, from the behaviour of the two single-absorbent systems just described, we can conclude that a CO₂ transfer improvement is likely to be observed when free PZ, and/or its carbamate, are present in the solution in a sufficient quantity, whereas the presence of MDEA alone has a negligible effect on this parameter.

The qualitative interpretation of raw data for the blends is obviously more complex but previous

observations will be used to reach reasonable conclusions. Again referring to the Figures 2A and 3A (ie, to the results of measurements carried out on the gas phase side), the CO₂ absorption rates in the blends can be roughly partitioned into two regions. From Figure 2, for example, we can see that for the first 8 hours the CO₂ flux decreases with time, rapidly for the first 2 hours and then less so for the remaining 6 hours. In this first region, at shorter times the trends of the absorbing fluxes pertaining to the mixture A and to PZ alone are not significantly different, whereas at intermediate times the mixture performance deviates markedly from the performance of PZ and MDEA. Finally, in the second region, after ~8 hours, the rate of absorption of the mixture stabilizes and becomes essentially equal to that of the MDEA alone. A similar behaviour, with different timing, is exhibited from mixture B (Figure 3).

The measured data provide general information on the kinetics of the system; however, they are unable to elucidate the involved mechanisms since they lump together different contributions to the absorption rate.

The system thermodynamics may help gain a basic understanding of the collected data. Chemical equilibrium can be assumed to prevail in the bulk liquid phase due to the low CO₂ transfer rates combined with the small specific area of the absorbing device (<1 m⁻¹). In order to estimate the liquid bulk concentrations of all chemical species, it is necessary to write and solve the eight non-linear equations relative to reactions (R7)-(R14).

$$K_i = \prod_j C_j^{\nu_{ij}} \quad (4)$$

where i refers to a specific reaction; j refers to a specific component; K the equilibrium constant; and C expressed as molarity and ν the stoichiometric coefficient matrix, which was done here with the help of MatLab software. In order to numerically determine the liquid composition according to this hypothesis, the equilibrium constants for reactions (R7)-(R14) at 25°C must be known. The same values selected in Part I were used here. For the

sake of simplicity, in order to estimate the component speciation the Kent and Eisenberg approach was adopted. This choice is discussed and justified in Part I.^[22] While discussing this subject, it is important to refer to the work of Cullinane and Rochelle.^[39] For a given liquid initial (unloaded) composition, component concentrations are estimated and reported as a function of the amount of CO₂ absorbed. It is a common procedure to express this amount as a CO₂ loading. It should be stressed here, however, that if for a single absorbent the definition of loading is unambiguous, this is not the case for absorbing blends. Specifically an overall CO₂ loading α can be used (as is most commonly done), defined as moles CO₂/mol (PZ⁰ + MDEA⁰), where subscript 0 refers to initial conditions, but in some specific case it would be more useful to introduce a more specific loading, such as PZ only (α_{PZ} = mol CO₂/mol PZ⁰) or MDEA only (α_{MDEA} = mol CO₂/mol MDEA⁰).

In Figures 4 to 6, CO₂ loading based on PZ only will be used, as it highlights how much CO₂ can be captured by solutions containing equal quantities of PZ with and without MDEA. Figure 4 shows an enlarged window on the system composition up to α_{PZ} = 0.8; for sake of clarity, some species whose concentrations are irrelevant have been omitted. Figure 4B sets an example for the specific case of blend A (PZ initial concentration = 0.116 kmol/m³, MDEA initial concentration = 0.844 kmol/m³). In Figure 4A, equilibrium speciation of PZ alone at the same initial concentration is also reported.

Figure 5A summarizes the concentrations of all CO₂ absorbed as PZ compounds taken from the calculated speciation data, including the two carbamates and the protonated monocarbamate at different loadings for the two systems, PZ alone and PZ + MDEA. It can be seen that for α_{PZ} between 0 and ~0.4, the two trends overlap and begin to diverge at α_{PZ} ≈ 0.5. For this value, the CO₂

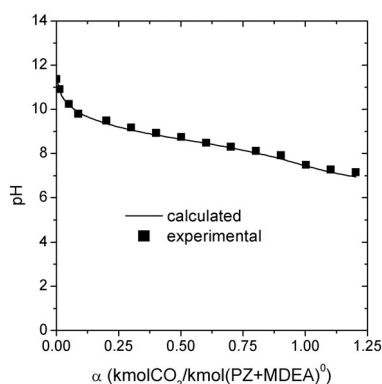


FIGURE 7 pH of blend A as a function of loading

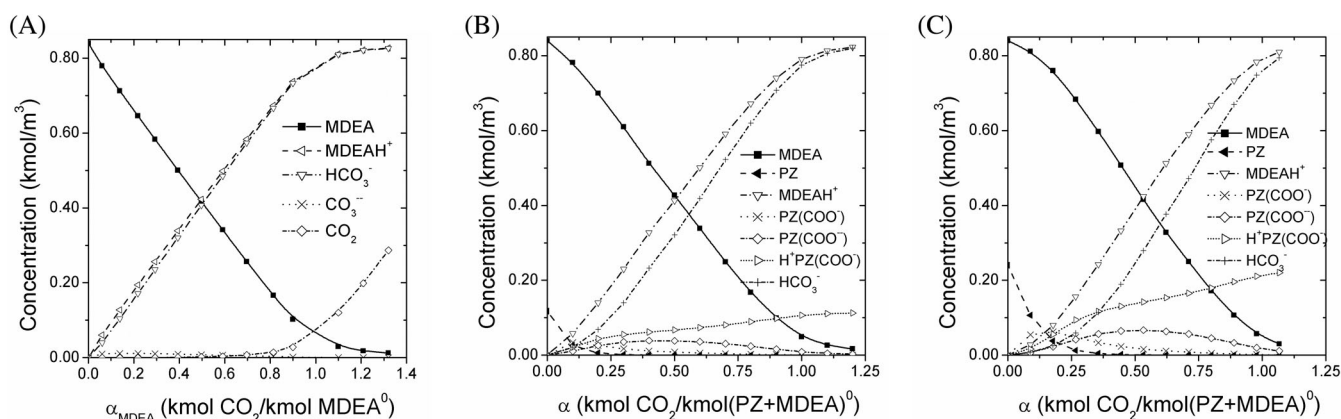
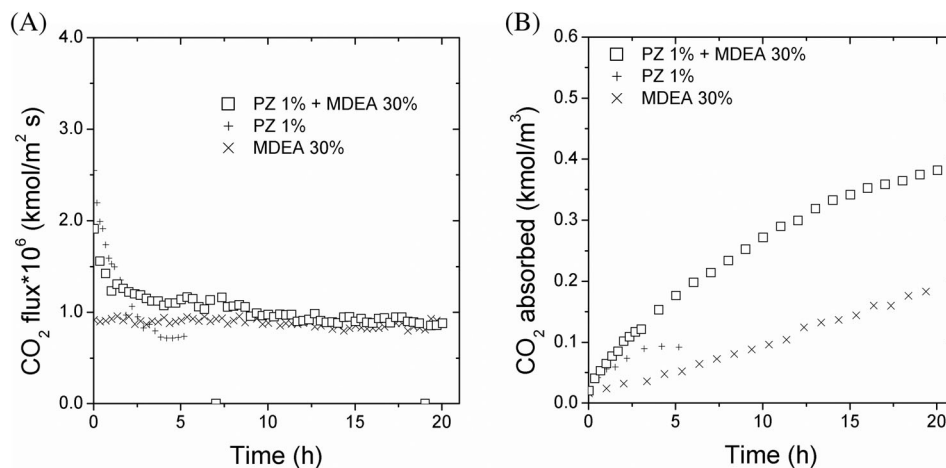


FIGURE 8 Component speciation in the bulk liquid phase for three different absorbing systems: A, MDEA 10%; B, MDEA 10% + PZ 1%; and C, MDEA 10% + PZ 2% at different loadings

FIGURE 9 CO₂ absorption performance of blend C with time



captured by the PZ species has a concentration of ~ 0.045 kmol/m³.

From Figure 5B, we can observe that at this ordinate the absorbing capacity of blend A becomes higher than that of PZ alone. This happens when roughly 2 hours have passed. As shown in Figure 5B, during this time span the absorbing fluxes of blend A and PZ are very similar; therefore, in this initial time interval only PZ seems to work as CO₂ absorbent.

Returning to Figure 5A, the slope of the blend A curve declines with loading and reaches a plateau at $\alpha_{PZ} \approx 2.2$, with a corresponding ordinate of 0.113 kmol/m³, which is a value virtually equal to the PZ initial concentration. Therefore, it can be concluded that at this point all the PZ initially present has reacted to capture CO₂ transforming itself in nonreactive forms, and henceforth only MDEA is active. Therefore, by adding MDEA the same quantity of PZ is used with maximum efficiency (100% vs $\sim 50\%$ for PZ alone) working for a longer time. The loading interval where MDEA supports PZ changes from $\alpha_{PZ} \approx 0.5$ to $\alpha_{PZ} \approx 2.2$, corresponding to a complete consumption of all PZ. In the absence of MDEA, due to thermodynamic constraints, the maximum possible loading value is 0.85, with a small amount of free PZ; however, there are significant amounts of monocarbamate and especially protonated piperazine still present in solution. Therefore, the speciation from the thermodynamic model predicts that the full absorption potential of PZ, if alone, cannot be totally expressed.

Based on the experimental results, Figure 5B shows that after 2 hours the blend performance improved and this improvement lasts over time, but gradually diminishes until a t_{max} at nearly 8 hours is reached. Here, the number of absorbed moles of CO₂ is ≈ 0.25 , and $\alpha_{PZ} = 0.25/0.116 \approx 2.2$, which is the same value identified in Figure 5A based on theoretical calculations. After t_{max} , the CO₂ fluxes obtained using the mixture or the MDEA

alone, and MDEA become essentially indistinguishable, and the number of moles of CO₂ captured increases steadily for mixture A and MDEA with essentially an equal slope. This signifies that in this time interval only MDEA is working, with the gas/liquid equilibrium not yet reached.

It is impressive that these findings match significantly even if they are derived from two independent approaches: the first being purely experimental and the second being theoretical (component speciation at the equilibrium in the bulk).

This behaviour can be explained through a deeper analysis of Figure 4. In the first loading zone, up to $\alpha_{PZ} \approx 0.4$ –0.5, by comparison with the case of PZ alone, for blend A we observe a similar amount of carbamate but a considerable depletion of PZH⁺ and a concomitant formation of an increasing quantity of MDEAH⁺. PZ, a stronger base, could be preferentially protonated after reaction (R11) (and (R12)); however, MDEA, present in a greater amount, will take over. It appears reasonable to hypothesize that the following equilibrium



which is a linear combination of (R10) and (R13) and can be considered instantaneous involving only a proton transfer, if present, will be largely shifted to the right. The interaction between the two reagents causes MDEA to make more PZ free, which otherwise would be in the protonated state. As a result, the fresh PZ becomes available to capture more CO₂ and at a faster rate, as also explicitly asserted by Puxty and Rowland.^[15] Indeed, the same authors demonstrated that a stronger base such as 2-amino-2-methyl-1-propanol (AMP) can have a more pronounced effect as it acts as a proton acceptor for a greater portion of the protons released upon the reaction between PZ and CO₂.

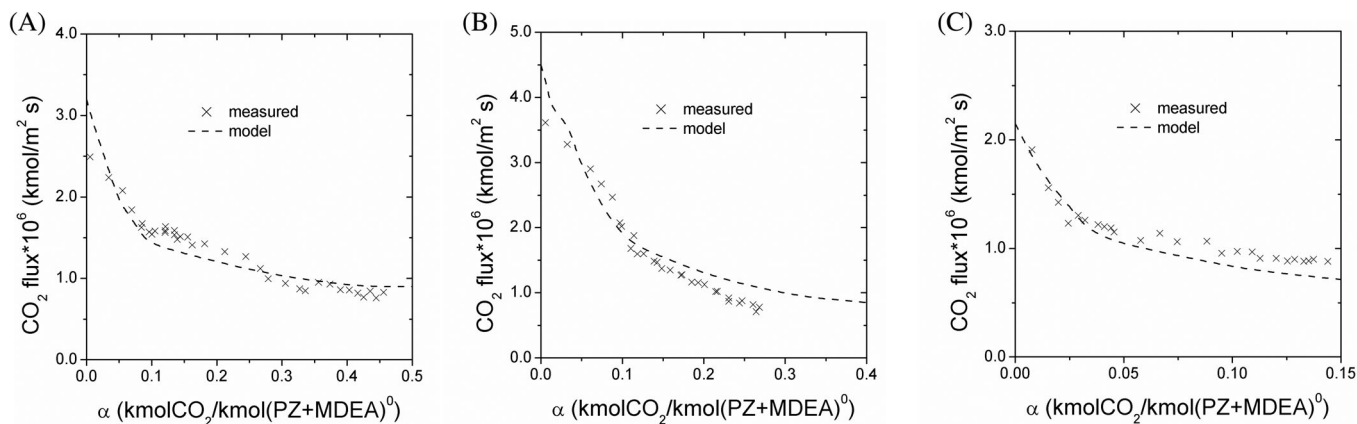


FIGURE 10 Measured and calculated CO_2 fluxes for the three systems investigated: A, system A; B, system B; and C, system C

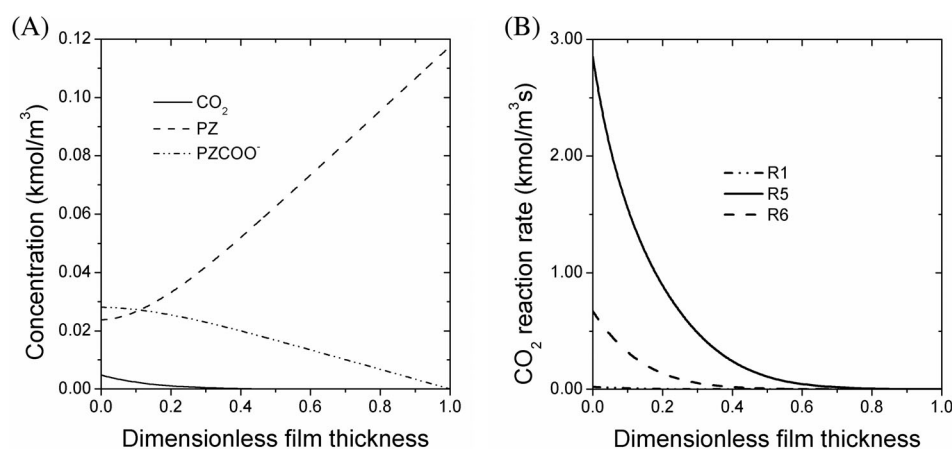


FIGURE 11 A, calculated concentration profiles; and B, CO_2 reaction rate in the liquid film.

$p_{\text{CO}_2} = 15 \text{ kPa}$; C_{bulk} (kmol/m³):
[MDEA] = 0.84, [PZ] = 0.118,
[PZCOO⁻] = 0

This effect, which becomes more important for $\alpha_{\text{PZ}} > 0.4$, would be felt only as long as protonated PZ and carbamate are available, that is, the interplay between PZ and MDEA operates until an $\alpha_{\text{PZ}} \approx 2.2$ is reached (t_{max} of ~ 8 hours), as explained above. Figure 4 shows that blend A [PZH⁺] has a maximum at $\alpha_{\text{PZ}} \approx 0.6$ –0.7 and then it declines. Conversely, no [PZH⁺] depletion is observable when PZ is alone. In this sense, MDEA helps PZ to work more effectively and efficiently and reach a higher absorbing capability.

For blend B (Figure 3), the discussion is similar; however, the beneficial effect of MDEA on PZ persists for a longer time, since the initial PZ concentration doubled. In this case t_{max} is detectable at nearly 13 hours, when $\sim 0.48 \text{ kmol/m}^3$ of CO_2 have been absorbed. The loading α_{PZ} is $0.48/0.233 \approx 2.1$, which is similar to the previous result. If a diagram analogous to that presented in Figure 5A is prepared (Figure 6), again the experimental results are confirmed by the theoretical speciation. The two trends (blend B and PZ 0.233 M) begin to diverge at $\alpha_{\text{PZ}} \approx 0.5$. For this value the concentration of the captured CO_2 can be interpolated to a value ≈ 0.095 – 1 kmol/m^3 , which is about twice the corresponding value of

Figure 5, as a double amount of initial PZ was present. The slope of the blend B curve reaches a plateau at $\alpha_{\text{PZ}} \approx 2.2$ again, with a corresponding ordinate of $\sim 0.23 \text{ kmol/m}^3$, which is equal to the PZ initial concentration in B.

At this point, a nonsecondary caveat must be stressed. It is implied that the accuracy of the predicted chemical speciation at equilibrium will depend on the accuracy of the parameters inserted in the system of equations detailed above. The reliability of the prediction can be partially assessed through the simple experimental measurement of the solution pH with the increase of the loading α . As an example, this is showed for blend A in Figure 7, where an unexpected excellent concordance between theoretical and experimental data can be observed. This fact encouraged us to put our trust in the results provided by the theoretical speciation diagrams.

Moreover, another important observation must be considered. In Part I,^[22] it was demonstrated that for a CO_2 -MDEA-water system the overall reaction (R15) can be used to describe the CO_2 absorption process. With the increase of the loading, concentrations of protonated MDEA and bicarbonate ions increase linearly and in

identical amounts, that is, $[\text{MDEAH}^+] = [\text{HCO}_3^-]$ continuously. In Figure 8, the theoretical equilibrium speciation for three different systems containing the same amount of MDEA (10%) yet different amounts of PZ (0%, 1%, 2%) is shown. In this figure, the loading is expressed as α_{MDEA} or α (see above).

In the first system (MDEA alone), with the increase of the loading, concentrations of protonated MDEA and bicarbonate ions increase linearly and in identical amounts. When 1% PZ is added, this does not happen; however, $[\text{HCO}_3^-]$ is noticeably lower than $[\text{MDEAH}^+]$. With PZ 2%, this discrepancy becomes even more marked. This is unequivocally due to the presence of PZ, which captures CO_2 under different forms (see the enhancement in carbamate and protonated carbamate and the disappearance of dissolved CO_2 moving from blend A to B to C).

The previous arguments are true also for blend C, but C exhibits its own characteristics (Figure 9). When the MDEA concentration is increased, the effect of the solution viscosity, which raises from $1.52 \text{ mPa} \cdot \text{s}$ (MDEA 10%) to $7.06 \text{ mPa} \cdot \text{s}$ (MDEA 30%), becomes immediately evident. CO_2 absorption is a process strongly influenced by the mass transfer resistance in the liquid phase. For blend C, at short time frames the absorption rate is noticeably lower than the absorption rate exhibited by the PZ alone, whose solution has a viscosity similar to that of pure water. Hence, by comparing Figures 2 and 9 (equal PZ initial concentration), a much less marked beneficial effect of MDEA on PZ is observable, that is, for mixture C the CO_2 capturing rate is far lower than the performance of blend A. This finding is due to a decrease in the k_L coefficient. t_{max} establishes here at ~ 10 hours, where the number of absorbed moles of CO_2 is ≈ 0.26 , and the corresponding loading, again in relation to PZ only, is $0.26/0.116 = 2.2$ of the same order of magnitude of the A and B mixtures.

In summary, the above discussion makes it unnecessary to invoke a PZ shuttle effect and seems to exclude the ability of PZ to continuously regenerate itself by a slow reaction in the bulk liquid, maintaining for the blend an enhanced absorbing performance that is sustained for a long time. Conversely, the blend performance decreases with time, and after a well-defined time span, and dependent on the initial PZ concentration, it becomes equal to that of MDEA because all the PZ and its carbamate are consumed.

5 | MODELLING

The qualitative findings reported and discussed in the previous section can be put on a quantitative footing and

the results can be compared with experimental observations. The main measured process parameter, CO_2 flux J from the gas stream to the liquid solution, will be examined.

The popular film approach is assumed valid in the description of the process, and mass transfer resistance in the gas stream is neglected as follows:

$$J_{\text{CO}_2} = \frac{p_{\text{CO}_2}}{\frac{1}{k_M} + \frac{H}{Ek_L}} \quad (5)$$

where p_{CO_2} is the CO_2 partial pressure in the gas phase; k_M represents an overall membrane gas transfer coefficient; H is the Henry constant; k_L is the liquid side mass transfer coefficient; and E is the enhancement factor for the CO_2 transfer in the liquid phase brought about by the chemical reactions. For the present setup, p_{CO_2} was fixed and always equal to 15 kPa, whereas k_M and k_L were experimentally determined, as reported in Part I,^[22] and equal to $1.0 \cdot 10^{-6} \text{ kmol}/(\text{m}^2 \cdot \text{s} \cdot \text{kPa})$ and $1.7 \cdot 10^{-4} (\eta/\eta_w)^{-0.33} \text{ m/s}$, respectively (η = solution viscosity, η_w = water viscosity).

Given that the Henry constant is easily retrievable from the open literature,^[22] only the numerical determination of the enhancement factor is needed to quantify the CO_2 flux. The present reacting system, made up of 12 components and eight reactions, is fairly complicated and E can only be estimated numerically for each condition. To this end, mass balance equations were written for the liquid film, with the pseudo-steady-state-hypothesis a reasonable assumption:

$$D_j \frac{\partial^2 C_j}{\partial x^2} + \sum_i r_{ij} = 0 \quad (6)$$

where j is the specific component; and i is the specific reaction. The different relationships necessary to estimate the diffusion coefficients are reported in detail in Part I.^[22] Boundary conditions for the film of thickness δ were as follows. At $x = 0$ (membrane-liquid interface), for every component j excluding CO_2 : $\frac{\partial C_j}{\partial x} = 0$ and for CO_2 : $C_{\text{CO}_2} = \frac{p_{\text{CO}_2,M}}{H}$, where $p_{\text{CO}_2,M}$ is the CO_2 partial pressure at the membrane-liquid interface. At $x = \delta$ (interface between liquid film and liquid bulk), $C_j = C_{j,b}$ is valid for every component, where $C_{j,b}$ is its concentration in the liquid bulk. As described earlier, bulk concentrations can be estimated by assuming thermodynamic equilibrium in the liquid phase.

The numerical solution of the system of differential equations requires the knowledge of each reaction rate. Previous works have investigated such reactions and suggested, for those involving CO_2 , that is, (R7), (R11), and (R12), identical kinetic laws of the following form.

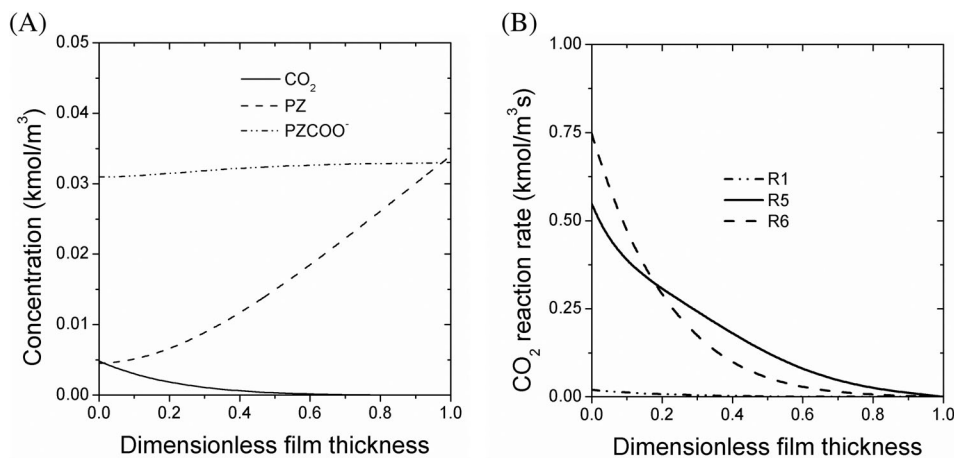


FIGURE 12 A, calculated concentration profiles; and B, CO₂ reaction rate in the liquid film. $p_{\text{CO}_2} = 15$ kPa; C_{bulk} (kmol/m³): [MDEA] = 0.84, [PZ] = 0.034, [PZCOO⁻] = 0.033

$$r_{\text{CO}_2} = -k_i C_B C_{\text{CO}_2} \quad (7)$$

where B represents MDEA, PZ, and carbamate for (R7), (R11) and (R12), respectively, and the kinetic constants at ambient temperature are equal to 5 m³/(kmol · s), 24 300 m³/(kmol · s), and 5600 m³/(kmol · s) respectively.^[40,38] All the other reactions were assumed to be instantaneous and at equilibrium. The numerical solution again was achieved with the help of Matlab routines. Details of the results are not presented here.

For each case considered, the concentration profiles were obtained for all the j components. CO₂ fluxes, with the relative enhancement factors, were calculated from the derivative of the CO₂ concentration profile at the membrane-liquid interface. The procedure just described was applied to all the three systems investigated, A, B, and C, and the results are depicted in Figure 10, comparing the predicted and the measured CO₂ fluxes. Considering the uncertainties related to the experimental measurements and those, even larger, related to the physical and chemical parameters necessary for the system description, the agreement is quite satisfactory, particularly because no fitting ad hoc parameters were introduced. This numerical simulation reinforces the conclusion reported in the previous section regarding the interaction between MDEA and PZ in the absorbing solution. Specifically, there is no need to introduce any further exotic chemical reaction to adequately describe the system behaviour.

Although no in-depth analysis of the numerical simulations is presented here, some basic considerations are discussed. In all the cases considered, the contribution of reaction (R7) to the CO₂ concentration profile in the film and therefore to the mass transfer enhancement was negligible, and this was fully expected given the difference in reaction rates when (R7) is compared to (R11) and (R12). As a matter of fact, as reported in detail in Part I,^[22] even when reaction (R7) is the only one taking place, little

effect on the CO₂ transfer is to be expected as the relative Hatta number is never larger than unity.

The comparative relevance of reactions (R11) and (R12) is less straightforward even if the kinetic constants differ by a factor of ~5. This is because carbamate, reactant for (R12), is also a product of (R11) and so prediction must take into account this aspect. Two specific cases will be presented and discussed here, the first referring to a system where only PZ is present in the absorbing solution (corresponding to unloaded solution) and the second where both PZ and carbamate are present in equal concentration (loaded solution).

Numerical simulations for the first case are represented in Figure 11 (A and B). In Figure 11A calculated concentration profiles for PZ, carbamate, and CO₂ are shown, whereas Figure 11B reports calculated reaction rate for reactions (R7), (R11), and (R12). It is evident that reaction (R12) contributes to CO₂ depletion by a factor that can be estimated as ~20% of the total. This conclusion is fully in line with previous numerical estimations, such as those from Onda et al.^[41] for systems with reactions in series.

Analogous results for the second case are reported in Figure 12. Here the contribution of the two reactions (R11) and (R12) to CO₂ capture is about equal, which is somewhat surprising given the difference in their rate constants. However, for the specific situation reported, reactions take place essentially in the half of the liquid film adjacent to the membrane, and PZ need to diffuse there in order to react, with a significant concentration drop, whereas carbamate is produced in the film through (R11) and does not need to diffuse from the bulk. The nearly flat profile resulting for the carbamate supports the conclusion that its diffusion is not a relevant factor.

It goes without saying that the contribution of (R12) becomes increasingly important as the carbamate concentration in the liquid bulk increases relative to PZ concentration.

Finally, it must be noted that the results presented and discussed here on CO₂ fluxes from the gas to the liquid phase depend heavily on the membrane characteristics. As already shown in Part I of this work,^[22] membrane resistance has little or no effect at low CO₂ transfer rates, where the main resistance lies in the liquid phase. However, as the fluxes increase due to the effect of the chemical reactions, the membrane becomes more and more influent, representing ~30% of the overall resistance to mass transfer. This aspect should be kept in mind when a comparison with other systems with different setups is carried out.

6 | CONCLUSIONS

This work deals with the process of CO₂ absorption from gas mixtures into MDEA-based aqueous solutions. In particular, the principal aim was to understand the reasons underpinning the noticeable improvement in the kinetics of the process brought about by the addition of small quantities of PZ. Three different blended absorbents containing different proportions of MDEA and PZ were experimentally and theoretically studied to this end.

In marked contrast to the assertions of several authors, our findings seem to exclude the ability of PZ to continuously regenerate itself by a slow reaction in the bulk liquid. In fact, the superior absorbing performance of the PZ/MDEA blends, compared to MDEA alone, lasts only for a limited time span.

We believe that the chemistry involved in the blend is not more complex than the chemistry associated with the two single reagents. In particular, a key factor to explain the enhanced mass transfer in the binary mixtures seems to be the role of MDEA as proton acceptor in place of PZ during the reactions leading to carbamate(s) formation. MDEA is a poorer base than PZ, but it is present at higher concentrations. The interaction between the two bases in the liquid film causes MDEA to release fresh PZ and the result is that more free PZ (or monocarbamate) is present in the solution, boosting the CO₂ absorption. Therefore, it is MDEA that enhances the action of PZ, in contrast to what many authors claim.

Our conclusions, well supported by experimental evidence and theoretical considerations, make it unnecessary to resort to a shuttle PZ effect. By shuttle mechanism, we mean the possibility of (slow) carbamate reversion to PZ in the bulk liquid and the back diffusion of the so-formed PZ to the interface. As a matter of fact, we find that during the saturation process the blend absorption rate decreases continuously with time. After a well-defined time span, dependent on the initial PZ concentration, the CO₂ flux flattens out, becoming equal to

that of MDEA. This evidence indicates that all the reactive forms of PZ have been definitively consumed.

REFERENCES

- [1] S. Mokhatab, W. A. Poe, J. Y. Mak, *Handbook of Natural Gas Transmission and Processing*, 3rd ed., Elsevier, Waltham, MA **2015**.
- [2] H. B. Liu, C. F. Zhang, G. W. Xu, *Ind. Eng. Chem. Res.* **1999**, 38, 4032.
- [3] S. Bishnoi, G. T. Rochelle, *Ind. Eng. Chem. Res.* **2002**, 41, 604.
- [4] Á. P. S. Kamps, J. Xia, G. Maurer, *AIChE J.* **2003**, 49, 2662.
- [5] R. Idem, M. Edali, A. Aboudheir, *Energy Procedia* **2009**, 1, 1343.
- [6] P. W. J. Derks, J. A. Hogendoorn, G. F. Versteeg, *J. Chem. Thermodyn.* **2010**, 42, 151.
- [7] H. Najibi, N. Maleki, *Fluid Phase Equilib.* **2013**, 354, 298.
- [8] S. K. Dash, S. S. Bandyopadhyay, *Int. J. Greenhouse Gas Control* **2016**, 44, 227.
- [9] L. Ghalib, B. S. Ali, W. M. Ashri, S. Mazari, I. M. Saeed, *Fluid Phase Equilib.* **2017**, 434, 233.
- [10] H. Suleman, A. S. Maulud, Z. Man, *Fluid Phase Equilib.* **2018**, 463, 142.
- [11] G. W. Xu, C. F. Zhang, S. J. Qin, Y. W. Wang, *Ind. Eng. Chem. Res.* **1992**, 31, 921.
- [12] X. Zhang, C. F. Zhang, S. J. Qin, Z. S. A. Zheng, *Ind. Eng. Chem. Res.* **2001**, 40, 3785.
- [13] S. Bishnoi, G. T. Rochelle, *AIChE J.* **2002**, 48, 2788.
- [14] R. H. Weiland, M. S. Sivasubramanian, J. C. Dingman, presented at 53rd Annual Lawrence Reid Gas Conditioning Conference, Norman, OK, February **2003**.
- [15] G. Puxty, R. Rowland, *Environ. Sci. Technol.* **2011**, 45, 2398.
- [16] A. Samanta, S. S. Bandyopadhyay, *Chem. Eng. J.* **2011**, 171, 734.
- [17] S. Mudhasakul, H. Ku, P. L. Douglas, *Int. J. Greenhouse Gas Control* **2013**, 15, 134.
- [18] A. Y. Ibrahim, F. H. Ashour, A. O. Ghallab, M. Ali, *J. Nat. Gas Sci. Eng.* **2014**, 21, 894.
- [19] A. Khan, G. N. Halder, A. K. Saha, *Int. J. Greenhouse Gas Control* **2017**, 64, 163.
- [20] M. Saidi, *Int. J. Chem. Kinet.* **2017**, 49, 690.
- [21] J. Ying, S. Raets, D. Eimer, *Energy Procedia* **2017**, 114, 2078.
- [22] C. Costa, M. Demartini, R. Di Felice, M. Oliva, P. Pagliai, *Can. J. Chem. Eng.* **2019**, 97, 1160.
- [23] P. Riou, P. Cartier, *Compt. Rend.* **1928**, 196, 1727.
- [24] D. H. Killeffer, *Ind. Eng. Chem.* **1937**, 29, 1293.
- [25] A. L. Shrier, P. V. Danckwerts, *Ind. Eng. Chem. Fundam.* **1969**, 8, 415.
- [26] H. Knuutila, O. Juliussen, H. F. Svendsen, *Chem. Eng. Sci.* **2010**, 65, 6077.
- [27] P. D. Vaidya, E. Y. Kenig, *Chem. Eng. Technol.* **2007**, 30, 1467.
- [28] G. Astarita, D. V. Savage, J. M. Longo, *Chem. Eng. Sci.* **1981**, 69, 581.
- [29] P. W. J. Derks, H. B. S. Dijkstra, J. A. Hogendoorn, G. F. Versteeg, *AIChE J.* **2005**, 51, 2311.
- [30] F. Khalili, A. Henni, A. L. L. East, *J. Chem. Eng. Data* **2009**, 54, 2914.
- [31] S. Bishnoi, G. T. Rochelle, *Chem. Eng. Sci.* **2000**, 55, 5531.
- [32] G. Capannelli, A. Comite, C. Costa, R. Di Felice, *Ind. Eng. Chem. Res.* **2013**, 52, 13128.
- [33] A. Comite, C. Costa, M. Demartini, R. Di Felice, M. Rotondi, *Int. J. Greenhouse Gas Control* **2016**, 52, 378.

- [34] A. Bottino, A. Comite, C. Costa, R. Di Felice, E. Varosio, *Sep. Sci. Technol.* **2015**, 50, 1860.
- [35] A. Comite, C. Costa, M. Demartini, R. Di Felice, M. Oliva, *Int. J. Greenhouse Gas Control* **2017**, 67, 60.
- [36] H. M. Stowe, E. Paek, G. S. Hwang, *Phys. Chem. Chem. Phys.* **2016**, 18, 25296.
- [37] J. J. Ko, M. H. Li, *Chem. Eng. Sci.* **2000**, 55, 4139.
- [38] W. Conway, D. Fernandes, Y. Beyad, R. Burns, G. Lawrance, G. Puxty, M. Maeder, *J. Phys. Chem. A* **2013**, 117, 806.
- [39] J. T. Cullinane, G. T. Rochelle, *Fluid Phase Equilib.* **2005**, 27, 197.
- [40] G. Astarita, D. W. Savage, A. Bisio, *Gas Treating with Chemical Solvents*, New York, Wiley **1983**.
- [41] K. Onda, E. Sada, T. Kobayashi, M. Fujine, *Chem. Eng. Sci.* **1970**, 25, 761.

How to cite this article: Costa C, Di Felice R, Moretti P, Oliva M, Ramezani R. Piperazine and methyldiethanolamine interrelationships in CO₂ absorption by aqueous amine mixtures. Part II—Saturation rates of mixed reagent solutions. *Can J Chem Eng.* 2020;1–14. <https://doi.org/10.1002/cjce.23820>